

Regulating Unified Power Quality Conditioner Output Using Kalman Filters

S. Mohana Priya¹, K. Keerthana²

^{1, 2}(P.G(PE&D) student, Asst Professor, Department of EEE, Dhanalakshmi Srinivasan Engineering College, Perambalur-12)

Abstract: This paper proposes a control design for the unified power quality conditioner (UPQC). This design, enabled by a control framework that employs the output regulation (OR) theory, is also made up of an Kalman filters used to extract the state components of the distorted supply voltage and load current, and as a state observer. In addition, the same framework integrates the major functions of the UPQC with ease to unify the treatments of several power quality problems including system harmonics in the supply voltage and load current, sags/swells in the supply voltage, variations in the load demands, and poor power factor at the supply side. A linear quadratic regulator-based self-charging circuit is incorporated into the control design so that the UPQC operates without relying on an external dc source. Simulation and experimental studies on a single-phase power distribution system are used to verify the performance and real-time implementation of this control design with the UPQC.

Index Terms: Harmonics compensation, Kalman filters, output regulation (OR), power quality, unified power quality conditioner (UPQC).

I. Introduction

NOWADAYS, the increasing use of nonlinear power electronics loads in industries [1] has led to harmonics generation. This poses great concerns for both the utilities and customers [2]. Voltage sags/swells in the supply voltage and poor power factor at the supply side also add to the number of power quality problems that the customers face [3]. As such, compliance with power quality standard, i.e., IEEE Standard 519, is pursued through the installation of compensating devices. Some of these devices that are able to resolve these power quality problems include the dynamic voltage restorers [4], [5], uninterruptible power supplies [6], active power filters [7]–[10], and unified power quality conditioners (UPQCs) [11], [12]. The UPQC is made up of the series and shunt active filters. It can be deployed in micro grids as well as in manufacturing plants like petrochemical plants and semiconductor plants that are dependent on a stable supply voltage. Recently, significant attention has been paid to the control circuit designs of the UPQC to obtain fast response so that the UPQC can tackle most of the power quality problems in a power distribution system and replace some of the power quality devices to reduce space and resources. To further handle the inherent coupling effects between the series and shunt active filters, a coordinated control for the UPQC is preferred. While ensuring robustness and efficiency, the deployment of the UPQC has to be cost effective to remain competitive. As such, modern control theories are used in the control design for the UPQC [13]–[19]. In view of the above issues, this paper presents an output regulation-based controller (ORC) [15], [20] with Kalman filters for the optimum operation of the UPQC. The ORC is used to generate control signals for the active filters of the UPQC in a coordinated manner. While the ORC ensures the global stability, it also facilitates periodic reference tracking and disturbance rejection so that a wide range of power quality problems can be concurrently handled in a power distribution system. The proposed UPQC has the following capabilities: 1) Harmonics compensation in the supply voltage and load current; 2) Compensation of sags and swells in the supply voltage; 3) Power factor correction at the supply side; and 4) Adaptive to the supply and load demand variations. The control design also includes 1) an exogenous Kalman filter to extract the fundamental and harmonic components of the supply voltage and load current; 2) a plant Kalman filter as a state observer for the variables of the UPQC; and 3) a linear quadratic regulator (LQR)-based self-charging circuit to regulate the dc-link voltage of the UPQC to a desired level. The exogenous Kalman filter, being part of the control design, also functions as a harmonic extractor, similar to the idea proposed in [18], [21]–[23]. Furthermore, this exogenous Kalman filter also facilitates selective filtering of the harmonic components [10], and is highly responsive to abrupt variations in the operating conditions, i.e., voltage sags or load demand variations. Utilizing the plant Kalman filter as a state observer also relaxes the requirement of numerous state measurements by sensors.

This results in a reduction in hardware circuitry, and manufacturing and maintenance costs. Simulation and experimental results for different operating conditions in a single-phase power distribution system are presented to validate the control design and its real-time performance.

II. Modeling of the Plant

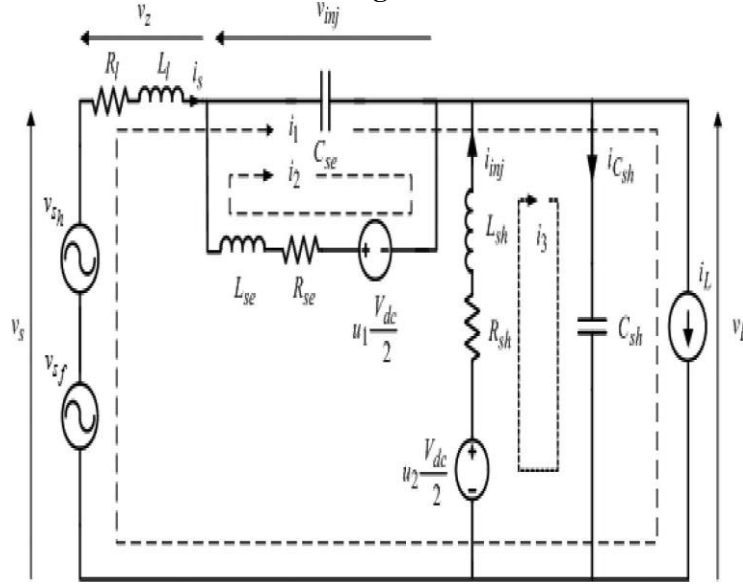


Fig. 1. Equivalent single-phase representation of the UPQC.

The equivalent single-phase representation of the UPQC in a power distribution system is shown in Fig. 1 [19]. The distorted supply voltage v_s at the point of common coupling is modeled by the sum of two voltage sources, namely, its fundamental v_{sf} and its harmonics v_{sh} . The nonlinear load is modeled by a distorted current source i_L , which is also made up of its fundamental i_{L_f} and its harmonics i_{L_h} that will change with different loadings. The supply current and the load voltage are denoted by i_s and v_L , respectively. Ideally, i_s and v_L should be sine waves of 50 Hz without any harmonic distortions, even though harmonics may exist in v_s and i_L . As such, this is one of the tasks to be accomplished by the UPQC. v_z in Fig. 1 models the voltage drop across the line impedance $R_l + j\omega L_l$.

$u_1(v_{dc}/2)$ and $u_2(v_{dc}/2)$ model the series and shunt active filters of the UPQC, respectively. Their associated low-pass interfacing filters and losses are modeled by L_{se} , C_{se} , and R_{se} and L_{sh} , C_{sh} , and R_{sh} , respectively. $i_{C_{sh}}$ is the leakage capacitor current of the shunt low-pass interfacing filter. $u_1(v_{dc}/2)$ and $u_2(v_{dc}/2)$ represent the switched voltages across the series and shunt VSI outputs of the UPQC, respectively. v_{inj} denotes the injected voltage of the series active filter, while i_{inj} denotes the injected current of the shunt active filter. u_1 and u_2 will be determined by the ORC to be discussed in Section III-C; they are supposed to take continuous values between -1 and +1. These continuous values will be modulated by PWM to become the switching signals for the VSIs. $(v_{dc}/2)$ is the desired voltage level of each capacitor unit for the UPQC.

Kirchhoff's voltage and current laws are applied to the three current loops indicated in Fig. 1 to derive a state space model for the UPQC.

From loop1,

$$v_s = i_1 R_1 + L_1 \frac{di_1}{dt} + v_{inj} + v_L \quad (1)$$

From loop2,

$$u_1 \frac{v_{dc}}{2} = R_{se} i_2 + L_{se} \frac{di_2}{dt} + v_{inj} \quad (2)$$

$$v_{inj} = \frac{1}{c_{se}} \int (i_1 + i_2) dt \quad (3)$$

From loop3,

$$u_2 \frac{v_{dc}}{2} - i_{inj} R_{sh} - L_{sh} \frac{di_{inj}}{dt} = v_L \quad (4)$$

$$i_s + i_{inj} - i_{C_{sh}} = i_L \quad (5)$$

In addition,

$$i_1 = i_s \quad (6)$$

$$i_2 = i_{se} \quad (7)$$

$$i_3 = i_{Csh} \quad (8)$$

where \mathbf{i}_{se} is the current flowing through \mathbf{R}_{se} and \mathbf{L}_{se}

Rearranging above equations the following state space representation for the plant and its state vector can be derived:

$$\begin{aligned} \dot{\mathbf{X}} &= \mathbf{A}\mathbf{x} + \mathbf{B}_1(v_s \ i_L)^T + \mathbf{B}_2\mathbf{u} & (9) \\ \mathbf{X} &= \begin{pmatrix} i_s \\ i_{se} \\ i_{inj} \\ v_{inj} \\ v_{csh} \end{pmatrix}; \quad \mathbf{A} = \begin{pmatrix} \frac{R_1}{L_1} & 0 & 0 & -\frac{1}{L_1} & -\frac{1}{L_1} \\ 0 & -\frac{R_{se}}{L_{se}} & 0 & -\frac{1}{L_{se}} & 0 \\ 0 & 0 & -\frac{R_{sh}}{L_{sh}} & 0 & -\frac{1}{L_{sh}} \\ \frac{1}{c_{se}} & \frac{1}{c_{se}} & 0 & 0 & 0 \\ \frac{1}{c_{sh}} & 0 & \frac{1}{c_{sh}} & 0 & 0 \end{pmatrix}; \\ \mathbf{u} &= (u_1 \ u_2)^T; \quad \mathbf{B}_1 = \begin{pmatrix} 0 & 0 & 0 & 0 & -\frac{1}{c_{sh}} \end{pmatrix}^T; \\ \mathbf{B}_2 &= \begin{pmatrix} 0 & 0 & \frac{v_{dc}}{2L_{sh}} & 0 & 0 \\ 0 & \frac{v_{dc}}{2L_{se}} & 0 & 0 & 0 \end{pmatrix}^T; \end{aligned}$$

And the output equation is given by,

$$\mathbf{y} = \mathbf{C}\mathbf{x} + \mathbf{D}_1(v_s \ i_L)^T + \mathbf{D}_2\mathbf{u} \quad (10)$$

where

$$\mathbf{C} = \begin{pmatrix} 0 & 0 & 0 & 0 & 1 \\ 1 & 0 & 0 & 0 & 0 \end{pmatrix}; \quad \mathbf{D}_1 = \begin{pmatrix} 0 & 0 \\ 0 & 0 \end{pmatrix}; \quad \mathbf{D}_2 = \begin{pmatrix} 0 & 0 \\ 0 & 0 \end{pmatrix}.$$

In this state-space model, the supply voltage v_s and the load current i_L are considered as exogenous inputs, which act like disturbances to the plant. The load voltage v_L and the supply current i_s are then considered as outputs of the plant, which are to be maintained as pure sine waves of 50 Hz, as well as to help in achieving a unity power factor at the supply side, to be discussed in Section III-A. The variables u_1 and u_2 are regarded as the control inputs to the plant. It is worth mentioning that the state-space model of the UPQC in (9) and (10) is a multi-input-multi-output system such that it does not treat the series and shunt active filters as two separate systems. Rather, a coordinated control is applied to operate the series and shunt active filters of the UPQC in a unified manner more effectively and efficiently.

Furthermore, since the distorted supply voltage v_s and the nonlinear load current i_L are considered as exogenous disturbances, the proposed control strategy also minimizes the negative effects of their variations. In addition, the active filters of the UPQC are made up of half bridge voltage source inverter. The sizing for the kVA capacity of the UPQC will depend on the functionalities of the UPQC.

For example, the functionalities of the MVR controlled UPQC are compensating capabilities in harmonics (in the supply voltage and load current) and disturbances in the supply voltage, and power factor correction at the supply side. In [11], the kVA capacities of the series and shunt active filters of the UPQC with similar functionalities are 7.5% and 2.5%, respectively, of the load capacity. As such, this principle may be applied generally and in the sizing of the active filters of the proposed UPQC in the paper.

III Control Philosophy

Next, this section discusses the formulation of the control design that aims to make the output of the plant $y = (v_L \ i_s)^T$ track a reference $r = (v_L^* \ i_s^*)^T$, under a periodic disturbance $(v_L \ i_s)^T$. The reference signals v_L^* and i_s^* are generally pure sine waves of 50 Hz without any harmonic distortions. Although various control strategies have been proposed for UPQC with some success, such as PI/PID [24], hysteresis control [13], [24], pole-shifting [25] and LQR/LQG [13], these methods do not guarantee that the steady-state error will be totally eliminated when the system is subjected to periodic references and disturbances. This paper proposes to apply the OR theory that utilizes a model of the reference and disturbance signals in the control design. In principle, this will provide a control configuration that can result in zero steady-state error. Furthermore, the proposed strategy treats the UPQC as a two input- two-output system directly, rather than two single input single- output systems as in some other methods. Thus, this will provide a more effective coordination of the two control variables u_1 and u_2 .

A. Construction of the Desired References

First, let v_s be represented by a Fourier series,

$$v_s = v_{sf} \sin \omega t + \sum_{h=3,5,\dots}^N v_{sh} \sin(h\omega t - \theta_{sh}) = v_{sf} + v_{sh} \quad (11)$$

Where v_{sf} denotes the fundamental component of v_s with amplitude v_{sf} . v_{sh} denotes the harmonic components of v_s , with amplitudes v_{sh} and phase angles θ_{sh} .

Then, from Fig. 1, (1) can be rewritten as

$$v_s = v_{sf} + v_{sh} = v_z + v_{inj} + v_L \quad (12)$$

Here, our objective is to regulate v_L to a clean sinusoidal voltage v_{sf} . As such, we fix v_L^* (the reference for v_L to track) to be v_{sf} , which is simply the first part of (12)

$$v_L^* = v_{sf} \sin \omega t = v_{sf} \quad (13)$$

In order to achieve this objective, the injected voltage v_{inj} will be

$$v_{inj} = v_{sh} + v_z = \sum_{h=3,5,\dots}^N v_{sh} \sin(h\omega t - \theta_{sh}) - v_z \quad (14)$$

where v_{inj} consists of v_{sh} for harmonics compensation in the supply voltage and v_z for compensating the voltage drop across the line impedance. After the initialization period of the UPQC, the amplitude of v_L^* is kept fixed to the predetermined amplitude of v_{sf} . In the event of a sag (or swell) in the supply voltage, v_s will be

$$v_s = (v_{sf} - \Delta v_{sf}) \sin \omega t + \sum_{h=3,5,\dots}^N (v_{sh} - \Delta v_{sh}) \sin(h\omega t - \theta_{sh}) \quad (15)$$

where Δv_{sf} and Δv_{sh} represent a corresponding sag in the amplitudes of its fundamental and harmonic components, respectively. For v_L to track v_L^* , the injected voltage of (12) will become

$$v_{inj} = -\Delta v_{sf} \sin \omega t + \sum_{h=3,5,\dots}^N (v_{sh} - \Delta v_{sh}) \sin(h\omega t - \theta_{sh}) - v_z \quad (16)$$

In (16), the first and second terms compensate for the voltage sag in the amplitudes of its fundamental and harmonic components, respectively. The third term compensates for the voltage drop across the line impedance. Likewise, let i_L be represented by a Fourier series

$$\begin{aligned} i_L &= I_{L_f} \sin(\omega t - \theta_{L_f}) + \sum_{h=3,5,\dots}^N I_{L_h} \sin(h\omega t - \theta_{L_h}) \\ &= I_{L_f} \sin \omega t \cos \theta_{L_f} - I_{L_f} \cos \omega t \sin \theta_{L_f} + \sum_{h=3,5,\dots}^N I_{L_h} \sin(h\omega t - \theta_{L_h}) \\ &= i_{L_{f,p}} + i_{L_{f,q}} + i_{L_h} \end{aligned} \quad (17)$$

where $i_{L_{f,p}}$ and $i_{L_{f,q}}$ are the load instantaneous fundamental phase and quadrature currents, which are always in phase and 90° out of phase with the supply voltage, respectively. I_{L_f} is the amplitude of i_L and θ_{L_f} is the phase angle difference between v_{sf} and i_{L_f} . i_{L_h} is the harmonic components of i_L , with amplitudes I_{L_h} and phase angles θ_{L_h} . From Fig. 1, (5) can be rewritten as

$$i_s + i_{inj} = i_L + i_{c_{sh}} = i_{L_{f,p}} + i_{L_{f,q}} + i_{L_h} + i_{c_{sh}} \quad (18)$$

In order for the shunt active filter of the UPQC to perform harmonics compensation and power factor correction concurrently, i_s^* (the reference for i_s to track) is set to be $i_{L_{f,p}}$

$$i_s^* = i_{L_{f,p}} = I_{L_f} \cos \theta_{L_f} \sin \omega t \quad (19)$$

In order to achieve (19), the injected current i_{inj} in (18) will be

$$i_{inj} = i_{L_{f,q}} + i_{L_h} + i_{c_{sh}} \quad (20)$$

where i_{inj} consists of i_{L_h} for harmonics compensation at the load side, $i_{L_{f,q}}$ for power factor correction at the supply side, and $i_{c_{sh}}$ for supplying the leakage capacitor current. The above construction of the desired references v_L^* , i_s^* can also be extended to selective harmonic filtering easily. For example, if the third, fifth, and seventh-order harmonic components of i_L may be excluded in the harmonics compensation, then i_s^* will be

$$i_s^* = i_{L_{f,p}} + i_{h_{SHC}} = I_{L_f} \sin \omega t \cos \theta_{L_f} + \sum_{h=3,5,\dots}^N I_{L_h} \sin(h\omega t - \theta_{L_h}) \quad (21)$$

where $i_{h_{SHC}}$ refers to the harmonic components of i_L that are not “selected” for harmonics compensation.

B. Modeling of the Exogenous Signals

Since all the exogenous signals v_s , i_L , v_L^* , i_s^* are periodic, they can be represented by a state-space model. For example, v_s in (11) can be represented by

$$\dot{\xi}_{v_s} = A_{v_s} \xi_{v_s} \quad (22)$$

$$v_s = c_{v_s} \xi_{v_s} \quad (23)$$

i_L , v_L^* , i_s^* can be modeled into a state-space form, although obviously the reference signals are sinusoidal, and their state vectors consist of two components only. All four state-space models can be combined into the following general form:

$$\dot{\xi} = \tilde{A} \xi \quad (24)$$

$$(v_s \ i_L)^T = \tilde{c}_w \xi + w \quad (25)$$

$$r = (v_L^* \ i_s^*)^T = \tilde{c}_d \xi \quad (26)$$

Which is called the exogenous system in this paper and w is the unmodeled harmonic components of $(v_s \ i_L)^T$. This state space model will be further discussed in Section III-D. The values of ξ , which are needed by the ORC in Section III-C, can be obtained by passing the measurable signals v_s and i_L into a Kalman filter designed for the state space model (24)–(26). Since estimating the state ξ is equivalent to extracting the fundamental and harmonic components of the exogenous signals v_s and i_L , the Kalman filter known as the exogenous Kalman filter in this paper serves as a replacement of the extraction circuit in conventional harmonics compensation designs. In some previous works of harmonics estimation [21]–[23], similar approaches of Kalman filtering have been adopted. The design of the exogenous Kalman filter will be discussed in Section III-D.

C. Output Regulation-Based Controller (ORC)

Substituting the exogenous system (24)–(26) into the state space model of the UPQC in (9) and (10), the following model obtained:

$$\dot{x} = Ax + B_0 \xi + B_2 u \quad (27)$$

$$y = Cx + D_0 \xi + D_2 u \quad (28)$$

The OR control law is then proposed as

$$u = U \xi + F(x - X \xi) \quad (29)$$

where u is the control signal generated by the controller as the switching scheme for the UPQC. x and ξ are the respective outputs of the exogenous and plant Kalman filters which will be discussed in the next section. The matrix gains U and X are computed from a pair of linear matrix equations called the regulator equations

$$X \tilde{A} = AX + B_0 + B_2 U \quad (30)$$

$$\tilde{C}_d = CX + D_0 + D_2 U \quad (31)$$

which will also transform the overall closed-loop system by multiplying (30) and (31) with ξ , subtracting them from (27) and (28) and then applying (24), (26) and (29) to become

$$\frac{d}{dt}(x - X \xi) = (A + B_2 F)(x - X \xi) \quad (32)$$

$$e = (C + D_2 F)(x - X \xi) \quad (33)$$

Where $e = y - r$ is the tracking error. Hence, if the matrix gain F is chosen such that $A + B_2 F$ is Hurwitz the closed-loop system is stable. In practice, e is satisfactorily small but nonzero due to the nonlinear effect of the PWM.

Therefore, this paper also adopts another Kalman filter called the Plant Kalman filter in this paper to estimate x , to be discussed in Section III-D

D. Exogenous and Plant Kalman Filters

Although the control law (29) is effective, it is a state feedback control law and assumes that both the exogenous state ξ and the plant state x are available. In reality, it is possible to measure the latter using sensors, since the plant is a real physical system. However, it is impossible to measure ξ directly since the exogenous system is actually a virtual system. Furthermore, even though it is possible to measure x , it might be undesirable to install so many sensors into the system since it will increase the cost. Without direct measurements of the

states ξ and x , a possible way to estimate them reliably is to use Kalman filters. The state estimates provided by the Kalman filters can then be utilized by the state-feedback control law(29).

The general theory of a Kalman filter can be summarized as follows. For a state-space model,

$$\dot{x} = Ax + Bu + v_x \quad (34)$$

$$y = Cx + Du + v_y \quad (35)$$

where u is the known input to the system, x is the unmeasurable state, y is the measured output, v_x is called the process noise, and v_y is called the measurement noise with zero means A Kalman filter, which estimates x based on the known input u and the measured output y , is given by

$$\hat{x} = A\hat{x} + Bu + L(y - C\hat{x} - Du) \quad (36)$$

where \hat{x} is the estimate of x , and the estimator gain L is determined from the solution to the Differential Riccati Equation

$$AP + PA^T - (PC^T + N)R^{-1}(PC^T + N)^T + Q = \hat{P} \quad (37)$$

$$L = (\hat{P}C^T + N)R^{-1} \quad (38)$$

where P is the steady-state error covariance.

Our exogenous system (24)–(26) constructed in Section III-B can be decomposed into two subsystems, one for $(v_s \ i_L)^T$ with the state-vector ξ_w and the other for the reference signal r with the state-vector ξ_d

$$\dot{\xi} = \tilde{A}\xi = \frac{d}{dt} \begin{bmatrix} \xi_w \\ \xi_d \end{bmatrix} = \begin{bmatrix} A_w & 0 \\ 0 & A_d \end{bmatrix} \begin{bmatrix} \xi_w \\ \xi_d \end{bmatrix} \quad (39)$$

$$(v_s \ i_L)^T = \tilde{C}_w\xi + w = [C_w \ 0] \begin{bmatrix} \xi_w \\ \xi_d \end{bmatrix} + w \quad (40)$$

$$r = (v_L^* \ i_s^*)^T = \tilde{C}_d\xi = [0 \ C_d] \begin{bmatrix} \xi_w \\ \xi_d \end{bmatrix} \quad (41)$$

If $(v_s \ i_L)^T$ is measured and a Kalman filter is applied to the first subsystem

$$\dot{\xi}_w = A_w\xi_w \quad (42)$$

$$\begin{bmatrix} v_s \\ i_L \end{bmatrix} = C_w\xi + w \quad (43)$$

the state ξ_w for $(v_s \ i_L)^T$ can be estimated, which actually consists of the fundamentals v_{sf}, i_{Lf} as well as the harmonics of v_s and i_L .

However, in order to obtain a smoother estimate (in case of sudden changes of load, etc.), a Kalman filter can also be applied here. Note that the second subsystem of the exogenous system may be written as

$$\dot{\xi}_d = A_d\xi_d \quad (44)$$

$$r = C_d\xi_d \quad (45)$$

The output equation above means that the Kalman filter estimates the state ξ_d by “measuring” the ξ_d deduced from the estimate of the state ξ_w . To be more exact, the first Kalman filter measures $(v_s \ i_L)^T$ to estimate ξ_w based on the first subsystem (42) and (43). From this $\dot{\xi}_w$ the corresponding ξ_d is computed. Then, this computed ξ_d is passed to the second Kalman filter to obtain a filtered version $\hat{\xi}_d$ based on the second subsystem (44) and (45). Combining $\dot{\xi}_w$ and $\hat{\xi}_d$, we form an estimate of the total exogenous state $\hat{\xi}$, which will be used by the statefeedback control law (29). These two Kalman filters mentioned above are collectively known as the exogenous Kalman filter in this paper. The application of the Kalman filter to the plant state x is more straightforward. This Kalman filter simply uses the known inputs of the plant v_s, i_L, u (i.e., the exogenous input as well as the control input, both of which are known) and the outputs of the plant v_L, i_s to estimate the state x . This is called the “plant” Kalman filter in this paper. The estimate \hat{x} will also be passed to the state-feedback control law (29) to calculate the control signal u . The tuning of the exogenous Kalman filter and the plant Kalman filter adopted in this paper is discussed here. The covariances of the measurement noise are first set to diagonal matrices properly matching the noise levels of the respective ensors measuring the signals. For the exogenous Kalman filter, the covariance of the process noise of each periodic signal measured is essentially a scalar matrix, and its relative magnitude to the covariance of the measurement noise is then adjusted to give a desired speed (transient response) of the exogenous state estimations. On the other hand, the adjustment of the covariance of the process noise for the plant Kalman filter involves more trial-and-errors to ensure that the poles locations of $A - LC$ are also satisfactory. In the end, the damping factors of all $A - LC$ poles are at least ten times of the fundamental frequency, and the damping ratios are at least 0.85.

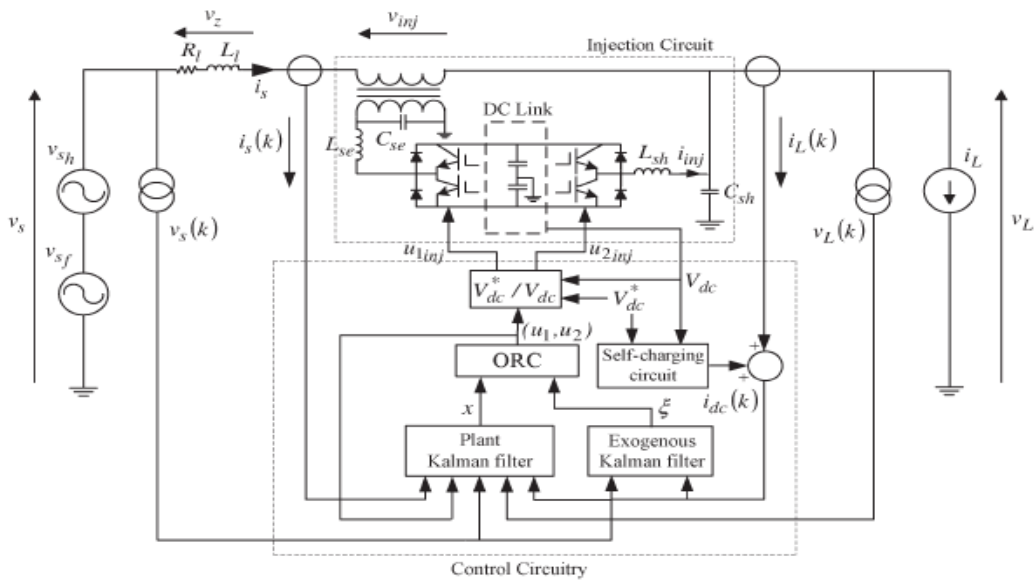


Fig. 2. State feedback ORC with Kalman filters as extraction circuit and state observer.

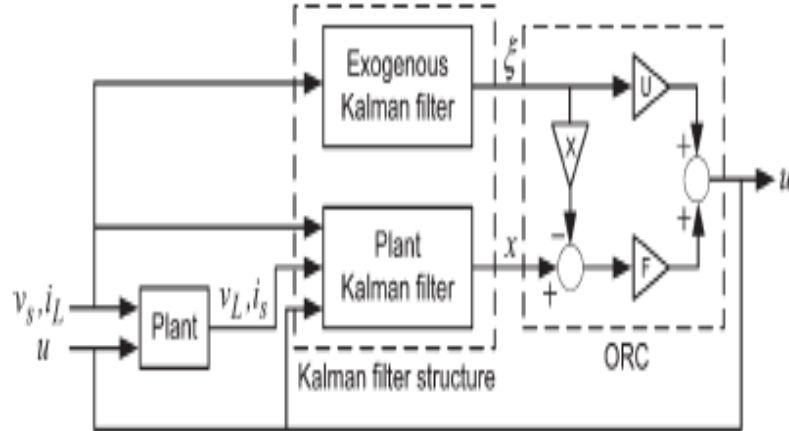


Fig. 3. System block diagram of UPQC with Kalman filters.

The matrix gains in both the Kalman filters and the control law (30), i.e., L , U , F , and X are all computed offline, and therefore their computational complexity is not an issue. In any case, they are obtained by solving some simple algebraic matrix equations.

In conclusion, by applying the exogenous Kalman filter and the plant Kalman filter, only four measurements, v_s , i_s , v_L , and i_L , are required. Indeed, these are the four variables that one would naturally choose to measure from the power system point of view. The control design is summarized in Fig. 2

E. Self-Charging Circuit

This paper proposes that the UPQC operates without relying on an external dc source. The supply side has to deliver additional real power through the shunt active filter to control the dc-link voltage. Here, a self-charging control design is proposed in Fig. 3 to meet this objective. Based on the conservation of energy, the effect of $I_{dc}(k)$ on the voltage $V_{dc}(k)$ of the capacitors in the dc link is given by

$$I_{dc}(k) = \frac{2C\left[\left(\frac{V_{dc}^*}{2}\right) - \left(\frac{V_{dc}(k)}{2}\right)\right]}{3VT} \quad (46)$$

where C is the value of each capacitor in the dc link, V is the peak amplitude of the supply voltage, and T is the period of the supply frequency. If v_{dc}^* denotes the desired dc voltage level of the dc link. Based on which a control law for $I_{dc}(k)$ is proposed

$$I_{dc}(k) = K_1 e_{dc}(k) + K_2 I(k) \quad (47)$$

where the gains K_1 and K_2 are optimized through the LQR theory [13], [19], which can provide better charging characteristics, e.g., no overshoot, fast settling time, than other conventional control design methods.

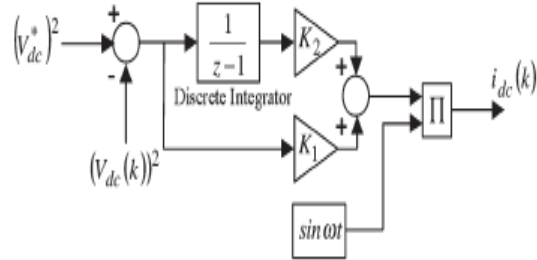


Fig. 4. LQR control topology for the regulation of the dc-link voltage of the UPQC.

IV. Injection Circuit

An injection circuit made up of VSIs and interfacing low pass filters shown in Fig. 3 is needed for the implementation of the control signals u_{inj} .

The injection circuit is made of

- 1) The UPQC which includes the series and shunt active filters,
- 2) A single-phase injecting transformer for interfacing the output of the series active filter with the distribution system,
- 3) The interfacing low-pass filters, and
- 4) Sensory circuits for the sampling of the required signals described in Section III.

The control signals generated by the control circuit will be the switching schemes for the respective active filters. Since u_{inj} takes continuous values from -1 to $+1$, they will be pulse width modulated as switching signals for the VSIs of series and shunt active filters of the UPQC. The VSI outputs then will be passed through the interfacing low-pass filters to eliminate the high switching frequencies.

V. Experimental Results

The control circuits making up of the ORC, the exogenous and plant Kalman filters, the self-charging and injection circuits described in the previous sections are connected together, and their performances are verified through simulation studies in Matlab. In the simulation studies, a single-phase distribution system of 1 kVA, 100 V_{rms}, 50 Hz with some nonlinear loads that include a single-phase dimmer load and a fluorescent lamp supplied by a distorted supply voltage typically found in a semiconductor plant is used for investigation. The dc-link voltage of the UPQC is 300 V. The exogenous state vector ξ in (25) consists of odd harmonics up to 29th order

The values of the various system parameters in Fig. 1 are given in Table I. The control design also requires the values of the line impedance and VSI impedances, which are coarsely estimated and listed in Table II. Since the latter values are not precisely known in practice, they become a source of modeling uncertainties for the control design to handle. Before the compensating capabilities of the UPQC are tested, the capacitors in the dc link have to be charged up. Thus, the first cycle will be used by the controller to charge v_{dc} to the desired level. Then, harmonics compensation is performed.

TABLE I
VALUES OF THE COMPONENTS OF THE UPQC

Component	V_{dc}	L_{se}	C_{se}	L_{sh}	C_{sh}
Value	300Vdc	3.8mH	10 μ F	1.8mH	10 μ F

TABLE II
LINE IMPEDANCE AND VSI IMPEDANCES OF THE UPQC

Component	R_l	L_l	R_{se}	R_{sh}
Value	0.01 Ω	1.0mH	0.01 Ω	0.01 Ω

TEST CASE 1: Harmonics Compensation in the Supply Voltage and Load Current with Power Factor Correction at the Supply Side

This test is performed to verify the capabilities of the UPQC to compensate for harmonics in the supply voltage and load current, and to achieve a near unity power factor at the supply side. The voltage and current waveforms under this condition are shown in Figs. 5 and 6, respectively. A distorted supply voltage v_s with a THD value of 60.4% is used to supply the dimmer load with a nonlinear current i_L shown in Fig. 6. i_L is also highly distorted with a THD value of 42.35% with a lagging power factor and consists of harmonics up to 13th order. With the installation of the UPQC and after the initialization period of less than two cycles, the waveforms of v_L (Fig. 5) and i_s (Fig. 6) are almost sinusoidal. The THD values of v_L and i_s drop to around 4.53% and 4.68%, respectively. During the steady state, it can be observed that the supply side only needs to deliver the real power demanded by the load and to maintain the dc-link voltage.

The reactive power delivered by the supply side is close to zero confirms that power factor correction to near unity is achieved at the supply side.

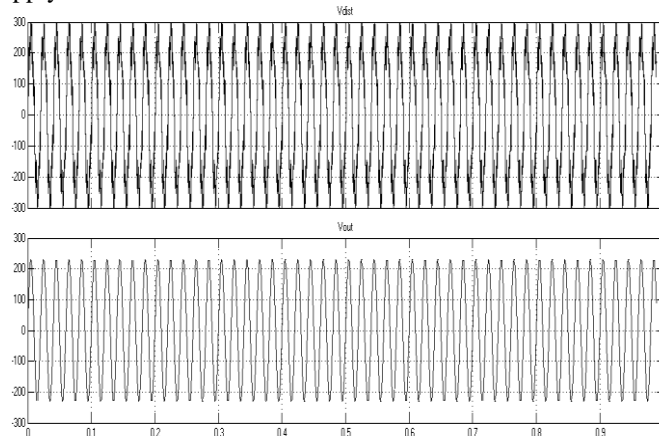


Fig. 5. Voltage waveforms under a distorted supply voltage with a nonlinear load.

During the steady state, it can be observed that the supply side only needs to deliver the real power demanded by the load and to maintain the dc-link voltage. The reactive power delivered by the supply side is close to zero. This confirms that power factor correction to near unity is achieved at the supply side. Fig.7 gives waveform of power factor showing unity. DC-link voltage value is maintained around 300V which is shown in simulation result fig.8

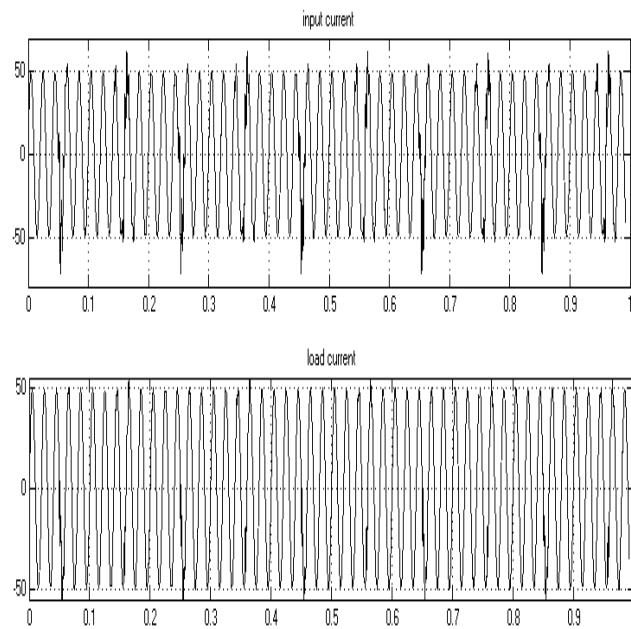


Fig. 6 Current waveforms under a distorted supply voltage with a nonlinear load.

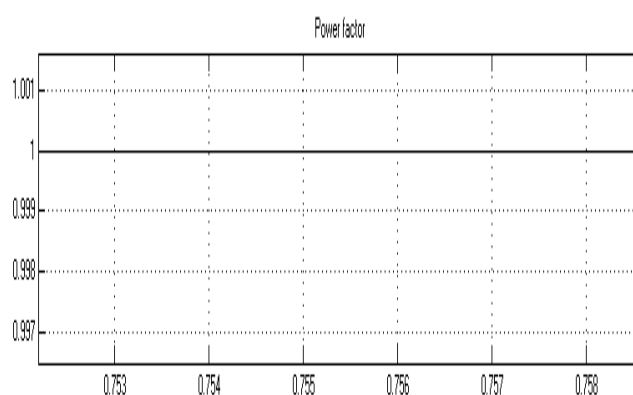


Fig. 7 Power Factor at supply side.

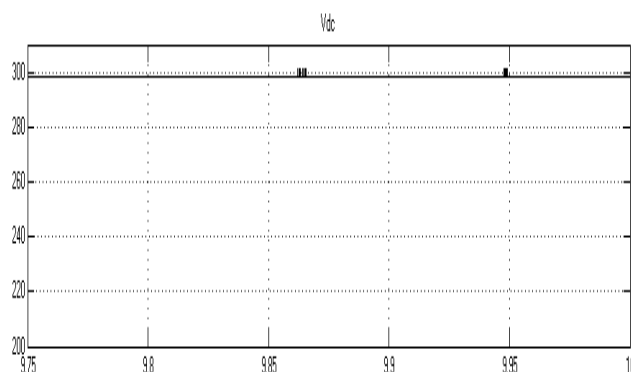


Fig. 8 DC-Link voltage

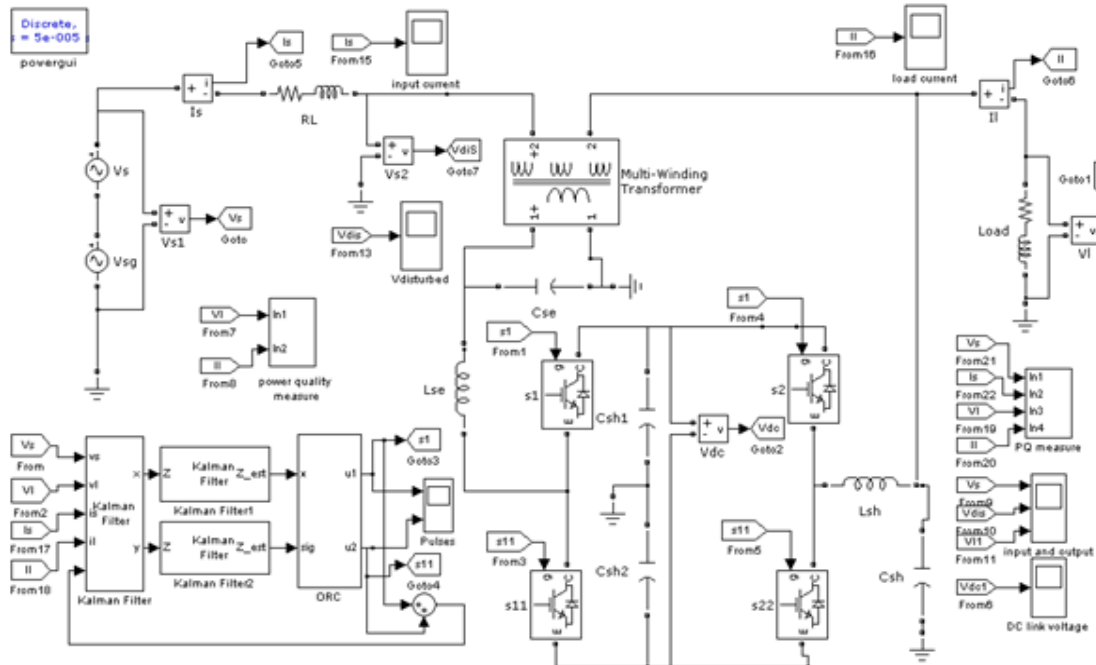


Fig. 9. Simulation diagram

V. Conclusion

A control design for the UPQC, which is adaptive to the variations of the supply and load operating conditions of a power distribution system, has been proposed. This control design consists of the ORC, the exogenous Kalman filters, the plant Kalman filter, and a LQR-based self-charging circuit. A self-charging circuit is incorporated into the control design so that the UPQC can operate without relying on an external dc source. The proposed control design is not only fast and adaptive but also cost effective for practical implementation and usage. Furthermore, the ORC can be applied to a three-phase power distribution system by duplicating three sets of the same controller, each of the controllers operating independently in the different phases to generate the switching sequence for the individual active filters of the UPQC.

REFERENCES

- [1] K. Chen, "The impact of energy efficient equipment on system power quality," in *Proc. IEEE Ind. Appl. Conf.*, 2000, vol. 5, pp. 3240–3247.
- [2] S. Ranade and W. Xu, "An overview of harmonics modeling and simulation," in *Tutorial on Harmonics Modeling and Simulation*. Piscataway, NJ: IEEE Power Eng. Soc., 1998, pp. 1–5.
- [3] A. Thapar, T. K. Saha, and Y. D. Zhao, "Investigation of power quality categorization and simulating its impact on sensitive electronic equipment," in *Proc. IEEE Power Eng. Soc. Gen. Meeting*, 2004, vol. 1, pp. 528–533.
- [4] J. D. Barros and J. F. Silva, "Multilevel optimal predictive dynamic voltagerestorator," *IEEE Trans. Ind. Electron.*, vol. 57, no. 8, pp. 2747–2760, Aug. 2010.
- [5] A. M. Massoud, S. Ahmed, P. N. Enjeti, and B. W. Williams, "Evaluation of a multilevel cascaded-type dynamic voltage restorer employing discontinuous space vector modulation," *IEEE Trans. Ind. Electron.*, vol. 57, no. 7, pp. 2398–2410, Jul. 2010.
- [6] D. E. Kim and D. C. Lee, "Feedback linearization control of three-phase UPS inverter systems," *IEEE Trans. Ind. Electron.*, vol. 57, no. 3, pp. 963–
- [7] L. H. Tey, P. L. So, and Y. C. Chu, "Improvement of power quality using adaptive shunt active filter," *IEEE Trans. Power Del.*, vol. 20, no. 2, pp. 1558–1568, Apr. 2005.
- [8] Z. Chen, Y. Luo, and M. Chen, "Control and performance of a cascaded shunt active power filter for aircraft electric power system," *IEEE Trans. Ind. Electron.*, vol. 59, no. 9, pp. 3614–3624, Sep. 2012.
- [9] Y. Tang, P. C. Loh, P. Wang, F. H. Choo, F. Gao, and F. Blaabjerg, "Generalized design of high performance shunt active power filter with output LCL filter," *IEEE Trans. Ind. Electron.*, vol. 59, no. 3, pp. 1443–1452, Mar. 2012.
- [10] S. Rahmani, A. Hamadi, and K. Al-Haddad, "A Lyapunov-functio based control for a three-phase shunt hybrid active filter," *IEEE Trans. Ind. Electron.*, vol. 59, no. 3, pp. 1418–1429, Mar. 2012.
- [11] H. Fujita and H. Akagi, "The unified power quality conditioner: The integration of series- and shunt-active filters," *IEEE Trans. Power Electron.*, vol. 13, no. 2, pp. 315–322, Mar. 1998.
- [12] H. Akagi, "New trends in active filters for power conditioning," *IEEE Trans. Ind. Appl.*, vol. 32, no. 6, pp. 1312–1322, Nov./Dec. 1996.

- [13] L. H. Tey, P. L. So, and Y. C. Chu, "Unified power quality conditioner for improving power quality using ANN with hysteresis control," in *Proc. IEEE Int. Conf. PowerCon*, 2004, vol. 2, pp. 1441–1446.
- [14] J. Munoz, J. Espinoza, E. Espinosa, C. Baier, P. Melin, L. Moran, and D. Sbarbaro, "Design of a discrete-time linear control strategy for a multicell UPQC," *IEEE Trans. Power Electronics*, 2011, to be published.
- [15] K. H. Kwan, P. L. So, and Y. C. Chu, "Unified power quality conditioner for improving power quality using MVR with Kalman filters," in *Proc. Int. Power Eng. Conf.*, 2005, vol. 2, pp. 980–985.
- [16] G. S. Kumar, B. K. Kumar, and M. K. Mishra, "Mitigation of voltage sags with phase jumps by UPQC with PSO-based ANFIS," *IEEE Trans. Power Del.*, vol. 26, no. 4, pp. 2761–2773, Oct. 2011.
- [17] V. Khadkikar and A. Chandra, "A novel structure for three-phase four wire distribution system utilizing unified power quality conditioner
- [18] K. H. Kwan, Y. C. Chu, and P. L. So, "Model-based $H\infty$ control of a unified power quality conditioner," *IEEE Trans. Ind. Electron.*, vol. 56, no. 7, pp. 2493–2504, Jul. 2009.
- [19] A. Ghosh and G. Ledwich, *Power Quality Enhancement Using Custom Power Devices*. Norwell, MA: Kluwer, 2002, pp. 380–406.
- [20] Z. L. Lin, A. A. Stoorvogel, and A. Saberi, "Output regulation for linear systems subject to input saturation," *Automatica*, vol. 32, no. 1, pp. 29–47, Jan. 1996.
- [21] J. A. Macias and A. Gomez, "Self-tuning of Kalman filters for harmonic computation," *IEEE Trans. Power Del.*, vol. 21, no. 1, pp. 501–503, Jan. 2006.
- [22] V. Moreno, A. Pigazo, and R. I. Diego, "Reference estimation technique for active power filters using a digital Kalman algorithm," in *Proc. Int. Conf. Harmon. Qual. Power*, 2002, vol. 2, pp. 490–494.
- [23] S. Liu, "An adaptive Kalman filter for dynamic estimation of harmonic signals," in *Proc. 1998 Int. Conf. Harmon. Qual. Power*, vol. 2, pp. 636–640.
- [24] Y. Kolhatkar and S. P. Das, "Experimental investigation of a single-phase UPQC with minimum VA loading," *IEEE Trans. Power Del.*, vol. 22, no. 1, pp. 373–380, Jan. 2007.
- [25] A. K. Jindal, A. Ghosh, and A. Joshi, "Interline unified power quality conditioner," *IEEE Trans. Power Del.*, vol. 22, no. 1, pp. 364–372, Jan. 2007.
- [26] P. C. Buddingh, "Even harmonic resonance-an unusual problem," *IEEE Trans. Ind. Appl.*, vol. 39, no. 4, pp. 1181–1186, Jul./Aug. 2003.